Tellus (2001), 53B, 380–393
Printed in UK. All rights reserved

TELLUS
ISSN 0280–6509

Chemical composition of aerosol during particle formation events in boreal forest

By J. M. MÄKELÄ[1,7]*, S. YLI-KOIVISTO[1], V. HILTUNEN[1], W. SEIDL[2], E. SWIETLICKI[3], K. TEINILÄ[4], M. SILLANPÄÄ[4], I. K. KOPONEN[1], J. PAATERO[4], K. ROSMAN[5] and K. HÄMERI[1,6], [1]*Department of Physics, PO Box 9, Siltavuorenpenger 20 D, FIN-00014 University of Helsinki, Finland;* [2]*Fraunhofer-Institute for Atmospheric Environmental Research, Kreuzeckbahnstrasse 19, D-82467 Garmisch-Partenkirchen, Germany;* [3]*Division of Nuclear Physics, Lund University, PO Box 118, S-221 Lund, Sweden;* [4]*Finnish Meteorological Institute (FMI), Air Quality Research, Sahaajankatu 20 F, FIN-00810 Helsinki, Finland;* [5]*Stockholm University (ITML), Air Pollution Laboratory, Institute of Applied Environmental Research, Stockholm University, S-10691 Stockholm, Sweden;* [6]*Finnish Institute of Occupational Health, Topeliuksenkatu 41 aA, FIN-00250 Helsinki, Finland;* [7]*Institute of Physics, Tampere University of Technology, PO Box 692, FIN-33101 Tampere, Finland*

(Manuscript received 15 May 2000; in final form 17 April 2001)

ABSTRACT

Size-segregated chemical aerosol analysis of a total 5 integrated samples has been performed for the atmospheric aerosol during events of new particle formation. The experiments were conducted during the BIOFOR 3 measurement campaign at a boreal forest site in southern Finland in spring 1999. Aerosol samples collected by a cascade low-pressure impactor were taken selectively to distinguish particle formation event aerosol from non-event aerosol. The division into "event" and "non-event" cases was done "in situ" at field, based on the on-line submicron number size distribution. The results on the chemical ionic composition of the particles show only small differences between the event and non-event sample sets. The event samples show lower concentrations of total sulfate and ammonium as well as light dicarboxylic acids such as oxalate, malonate and succinate. In the event samples, nucleation mode particle MSA (methanesulphonic acid) was found to be present exceeding the concentrations found in the non-event samples, but at larger particle sizes the sample sets contained rather similar concentrations of MSA. The most significant difference between the event and non-event sets was found for dimethylammonium, ionic component of dimethylamine ($(CH_3)_2NH$), which seems to be present in the particle phase during the particle formation periods and/or during the subsequent particle growth. The absolute event sample dimethylamine concentrations were more than 30-fold greater than the non-event concentrations in the accumulation mode size range. On the other hand, the non-event back-up filter stage for sub-30 nm particles contained more dimethylamine than the event samples. This fractionation is probably a condensation artifact of the impactor sampling. A simple mass balance estimate is performed to evaluate the quality and consistency of the results for the overall mass concentration.

1. Introduction

Ambient new particle formation and subsequent growth has been observed in several locations, based mostly on instrumentation to measure particle number related quantities (Weber et al., 1997; Mäkelä et al., 1997; O'Dowd et al., 1999). However, no chemical characterization of nucleation burst particles has been carried out previously. Thus, the chemical compounds involved in the nucleation and condensation processes have

* Corresponding author.
e-mail: jyrki.makela@helsinki.fi

not yet been experimentally identified. The general problem in the sampling for size-segregated chemical analysis of the aerosol is the amount of material required for the sample (usually in the order of more than tens of ng/m^3). This, automatically, sets the sampling times to be long e.g. with respect to the time scale of the nucleation bursts observed in the ambient air.

Size-segregated aerosol chemistry of fine particles ($Dp < 1$ μm) has been previously discussed in several papers. Conventionally, the main chemical components studied in the aerosol phase have been ionic sulfates, nitrates and other inorganic ionic species such as Na^+, Cl^-, NH_4^+, etc. Only recently, chemical size distributions of different hydrocarbons such as dicarboxylic acids (Jaffrezo et al., 1998; Teinilä et al., 2000; Kerminen et al., 1999) and pinonic acids (Kavouras et al., 1998) have been presented for ambient submicron particles.

Kavouras et al. (1998) presented chemical analysis of the particles smaller than 500 nm in connection with the increase of the Aitken nuclei in a forested area. They found pinonic acids to be present, which are known to be formed as oxidation products of gaseous monoterpenes emitted from the forest. However, size fractionated analysis of finer sized particles connected to the nucleation bursts have not been made so far.

The size of the particles being small, it is very difficult to analyze the aerosol material chemically. Also, complete segregation of the newly formed nucleation mode particles from the rest of the aerosol is difficult without having few large particles to contaminate the samples. In the recent impactor techniques, reliable segregation of particles below 30–50 nm may be possible. Usually the rest of the aerosol is removed by impactor stages and the nucleation mode particles may be collected on a back-up filter in the end of the cascade impactor. If aerosol mass is studied and chemically analyzed, we may have a chance to determine the species involved in the growth process of the particles subsequent to their formation, but there would hardly be a possibility to determine the species involved in the original nucleation process taking place, occurring already before the particles are seen to enter the lower boundary of measurement size range of Condensation Particle Counters (CPC) or Differential Mobility Particle Sizers (DMPS).

During the BIOFOR project, the formation of new particles as well as the overall dynamics of submicron particles were intensively studied (Kulmala et al., 2001). This paper describes the attempt to directly analyze the aerosol particle composition during the new particle formation events. Special effort is paid to focus on the differences of the chemical composition during and outside the nucleation bursts.

2. Experimental

The aerosol sampling for the study was performed within the BIOFOR 3 intensive measurement field campaign at Hyytiälä southern Finland (61° 51′ N, 24° 17′ E). The field station is located in boreal forest and represents background area of southern Finland. The measurement site as well as the location of the various instruments is discussed in detail in Kulmala et al. (2001). The BIOFOR 3 campaign was conducted during 29 March–27 April 1999 with 13 particle formation events observed during a period of 30 days. The instrumentation for aerosol mass sampling consisted of standard EMEP-filters (European Monitoring and Evaluation Programme), 2-stage Nuclepore filters, several cascade impactors and a TEOM. The sampling was done mostly on daily basis. Two multistage impactors were also used to sample aerosol during and outside the nucleation events. This sampling strategy is discussed more detailed in Section 3. Additionally, the data from differential mobility particle sizer (DMPS) was used on line to judge whether an aerosol formation event was taking place. The instrument characteristics are summarized in Table 1.

For chemical analysis the DLPI impactor samples (25-mm polycarbonate foils plus a 47-mm "Teflon" membrane back-up filter with pore size of 2 μm) were extracted into deionized ultra-pure water. Before extraction the filters were subjected to methanol liquid (10% of the total liquid) in order to enhance the extraction efficiency. The anions were analyzed by a Dionex DX-500 ion chromatography (IC) and the cations by a Dionex DX 100 IC (Kerminen et al., 1999). Samples were injected manually using a 1000-μl loop in Dionex DX-500 and a 300-μl loop in Dionex DX-100. The run time was 11 min in both cases.

The ion chromatographic method used for

Table 1. *Instrumentation for determination of particle mass and chemical composition during BIOFOR 3*

Instrument	Characteristics	Sampling period
DLPI impactors	13 stages + back filter ($\sim$5–30 nm)	event/non-event sampling
SDI impactors	multistages (Maenhaut et al., 1996)	24 h sampling
PM-10 impactors	3 stages: below 2.5 μm; 2.5–10 μm; above 10 μm	24–72 h sampling
filters	2 stages: cut size $\sim$1 μm	24 h sampling
EMEP filter	2 stages: particle filter + NaOH impregnated back filter for SO_2	24 h sampling
TEOM	total mass: inlet cut size $\sim$10 μm	30 min cycle
DMPS	twin DMPS set-up: 3–500 nm	10 min cycle

impactor stage analysis has been described by Teinilä et al. (2000). The ions determined were Na^+, NH_4^+, dimethylammonium ($(CH_3)_2NH_2$), K^+, Ca^{2+}, Mg^{2+}, SO_4^{2-}, NO_3^-, Cl^-, methanesulfonate acid (MSA^-), oxalate ($C_2O_4^{2-}$), malonate ($C_3H_2O_4^{2-}$) and succinate ($C_4H_4O_4^{2-}$). The field blank concentrations were relatively small compared to the concentrations in the actual samples. The blank concentrations were highest for sodium and calcium, but were still less than 10% of the sample concentrations. For dimethylamine the blank concentrations were below 5% of the maximum sample concentration. For carboxylic acids the blanks were below detection limit. The sensitivity of the chemical analysis of the cascade impactor foils can therefore be estimated to be of the order of 1–5 ng/m^3. For malonate and succinate the errors are higher, of the order of 30–50%, even though the blank concentrations were zero in this case. For identification of the compounds, also the less common ones such as dicarboxylic acids and the dimethylamine, analyzing standards have been used. The identification of compounds was based on the retention time in the IC column.

The collected EMEP filters were extracted for 30 min in a shaker with 10 ml of ultra-pure water. The extracts were filtered through 0,45 μm pore-size membrane filters and analyzed by ion chromatography using standard methods (EN ISO 10304-1, ISO 14911). As a part of the quality control procedure synthetic internal quality control samples were measured in every analyzed sample batch and their results were examined to be within the established control limits. Anions (chloride, nitrate, sulfate) and cations (sodium, ammonium, potassium, calcium and magnesium) were measured from the extracts of the front filters. Sulfur dioxide was measured as sulfate from the extracts of the impregnated back-up filters. Anions were analyzed using sodium gluconate-borate as a mobile phase. EDTA eluent was used for cation measurements. The SDI impactor samples were analyzed similarly.

Gravimetric analysis was performed for DLPI stages, the 2-stage filters and the PM-10 impactor stages with accuracy of 1–2 μg. The weighing was done at Hyytiälä site in a room with fairly constant temperature of approximately 20°C $\pm$ 2°C and relative humidity 50% $\pm$ 5%.

3. Sampling strategy for the event/non-event impactor

In our field experiment, the occurrence of the particle formation events was determined based on the DMPS data shown in Figs. 1a, b. The decision to start sampling was based in on-line analysis of the number size distribution. As the nucleation mode particles appeared and it seemed that a nucleation burst was starting, the event impactor was started to sample. If there was

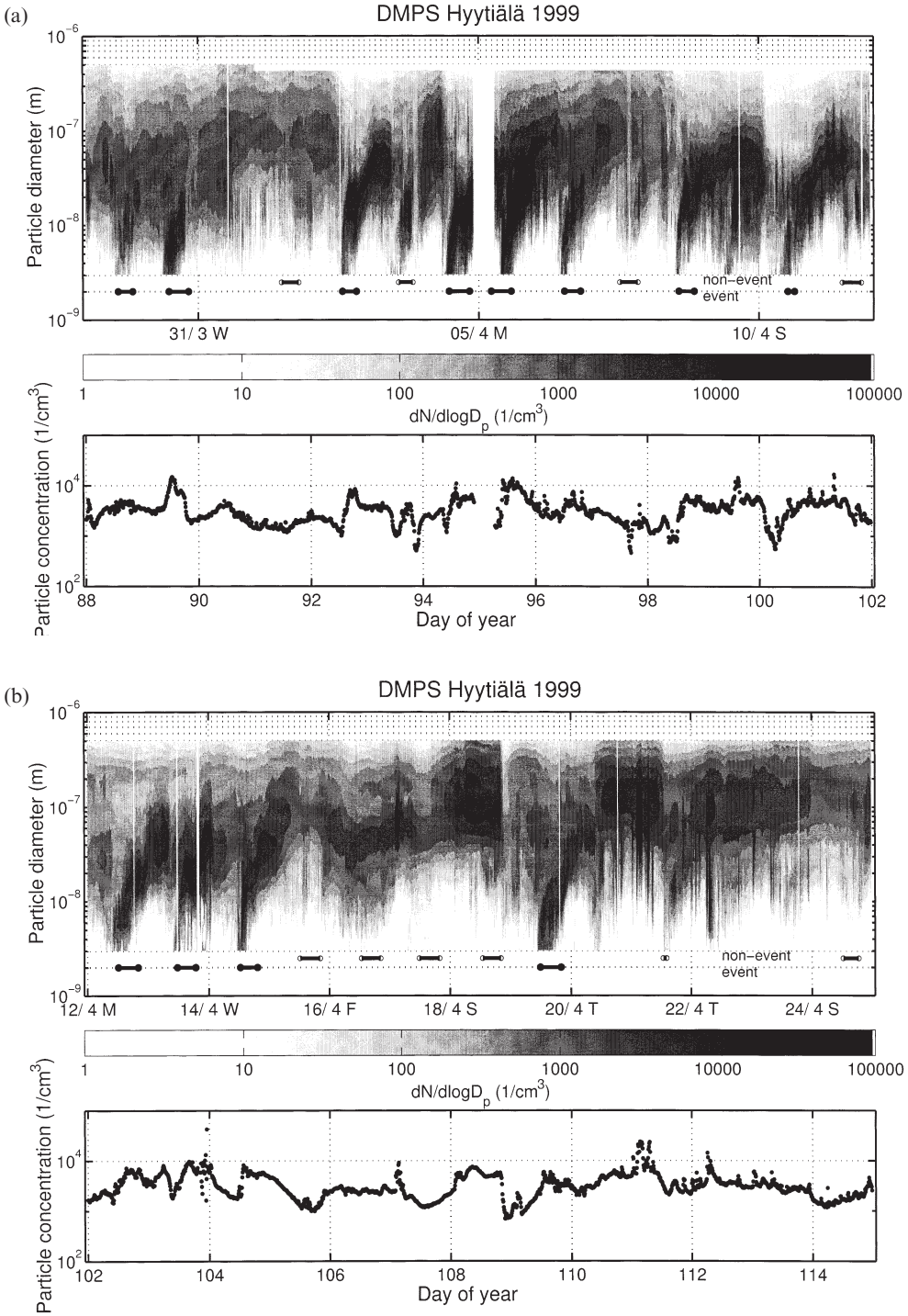

Fig. 1. Submicron particle number size distributions (3–500 nm) along with total particle number concentration derived from the differential mobility particle sizer (DMPS) spectra for the study period in Hyytiälä. The event/non-event cascade impactor sampling strategy is shown with horizontal bars in each distribution plot (upper row non-events; lower row events). The sampling took place always during afternoons, and the decision for the individual impactor to be used was done in field based on the DMPS-data.

reason to expect nucleation event not to take place (e.g., general meteorological conditions) the non-event impactor was started. In order to get sufficient mass, every impactor sample was taken over multiple periods. All together, there were 3 event samples (E1, E2, and E3) and 2 non-event samples (N1, N2). The periods when each of these samples was taken are indicated as horizontal bars added into the spectral plots (Figs. 1a, b). The upper gray bars refer to the non-event sampling periods and the lower black bars refer to the event sampling periods, respectively. The sampling was usually continued until 8–9 p.m. On the event days the stopping time slightly depended on the existence of the post event Aitken mode. From Figs. 1a, b it is apparent that practically all the particle formation bursts during the campaign were captured by the event impactor. The non-event samples were collected mostly during non-event periods, maybe excluding 3 April (DOY 93). 3 April may be considered an unclear case, since obviously a fairly high concentration of 10 nm particles can be seen to be present during the sampling period.

A closer description of the sampling schedule with some information about the air mass characteristics is presented in Table 2. The event samples E1 and E2 consist of air masses arriving mostly over Sweden (west–northwest), and have been classified as Arctic air mass with cold air advection, whereas the non-event sample N2 represents air masses arriving mostly over Baltic countries and St. Petersburg. The remaining samples E3 and N1 may be considered as mixtures of air masses arriving from several directions. The contribution from Tampere, a city 60 km southwest of Hyytiälä, is mentioned in the table, being practically the only local source of pollution in addition to Hyytiälä station itself, locating west–southwest from the measurement site.

Table 2. *A list of the event/non-event impactor collection arrangement in BIOFOR 3 during 29 March–27 April 2000 in Hyytiälä, accompanied by minor meteorological characteristics of the air masses on each day*

Date 1999	Day of year	Event (E)/ non-event (N) impactor, run #	Trajectory/ air mass
29 March	88	E1	Tre, Swe/AC
30 March	89	E1	Tre, Swe/AC
31 March	90	N1	Tre, Denm/S
1 April	91	N1	Tre, Denm/PC
2 April	92	E2	Swe Oslo/PC
3 April	93	N1	Norway, Gr/PC
4 April	94	E2	Norway, Gr/AC
5 April	95	E2	Norway, Gr/AC
6 April	96	E2	Tre, Swe/AC
7 April	97	N1	Tre, Swe/P
8 April	98	E2	Swe, Scot/AC
9 April	99	—	—
10 April	100	E2	Swe, Atl/AC
11 April	101	N1	Swe, Atl/P
12 April	102	E3	Norway, Atl/AC
13 April	103	E3	Lapl, Barents/AC
14 April	104	E3	St.Pet, Lapl/AC
15 April	105	N2	St. Pet, South/P
16 April	106	N2	Estonia, Pol/AC
17 April	107	N2	Estonia, Pol/A
18 April	108	N2	St. Pet, BLR/P
19 April	109	E3	Est, BLR/PC
20 April	110	—	—
21 April	111	N2	St. Peter, Rus/S
22 April	112	—	—
23 April	113	N2	Baltic, Ger/P
24 April	114	N2	Baltic, Ger/PC
27 April	117	E3	Baltic, Swe/P

Abbreviations used for the incoming air mass directions: Tre = Tampere, Swe = Sweden, Denm = Denmark, Gr = Greenland, Scot = Scotland, Atl = Northern Atlantic, Lapl = Lapland, St. Pet = St. Petersburg, Pol = Poland, BLR = Belarussia, Est = Estonia, Ger = Germany. Abbreviations for the air mass description (see Nilsson et al., 2001): AC = Arctic/Cold air advection, S = Subtropical, P = Polar, PC = Polar/Cold air advection.

4. Number size distributions

To estimate the presence of particles of different sizes during the event/non-event sampling, we have calculated the averaged number size distributions from DMPS for the 5 separate samples E1, E2, E3, N1 and N2. As a result of the averaging, we obtain 5 average number size distributions to describe the 5 mass distribution samples. The averaged number size distributions, presented in Fig. 2, show again that the collection strategy has been quite successful. The first event sample E1 contains a clear number mode at 7–8 nm, whereas for E2, the nucleation mode is located approximately at 15 nm. It is clear, that along with the particle growth subsequent to the particle forma-

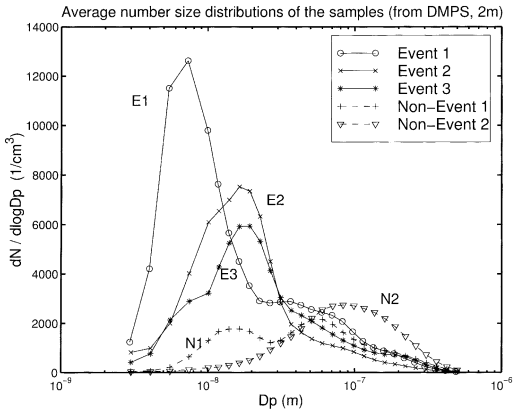

Fig. 2. Averaged submicron particle number size distributions during each cascade impactor sampling period. The non-event 1 sample (N1) contains a clear mode of 15 nm particles, whereas the event 2 (E2) sample consist of periods with relatively low concentration of accumulation mode particles.

tion burst, the averaged nucleation mode should automatically shift towards larger sizes. The same is seen for the E3 sample as well. Non-event 2 seems to be a clear non-event sample having no trace of nucleation mode particles. The nucleation mode showing up in non-event 1 arises from 3 April which, slightly erroneously, was categorized as a non-event day at the field. Looking back at the DMPS-data, a clear nucleation mode exists on that day. However, the nucleation mode particles appear into the DMPS spectra being already more than 10 nm in size. 3 April can be considered as the only day when the sampling strategy slightly failed. All in all, the data can be considered successful in separating the event and non-event aerosol.

5. Mass concentrations and mass size distributions

The particle mass concentration levels in Hyytiälä are typically around 5–50 μg/m^3, the fine particle mass being typically in the order of 2–20 μg/m^3. Highest fine particle mass concentrations are usually observed when the air masses arrive from south or southwest. The fine particle mass ($Dp < 1$ μm) from the 2-stage filters along with the PM-2.5 mass concentrations determined by the Dekati PM-10 impactor are presented in Fig. 3 for the BIOFOR 3 campaign period. Note that the filter collection has been performed as daily samples but the PM-10 impactor was running on 2–3-days periods (3 samples per week). The first part of the campaign was a cleaner period with a fine particle mass of 4–8 μg/m^3, whereas the second part starting from 15 April 1999 (DOY 105) along with N2 samples, elevated mass concentrations in the order of 10–15 μg/m^3 were obtained. The fine particle mass concentrations obtained by the two independent, but not identical, methods agree within ±30–50%.

All the mass size distributions measured by DLPI, shown in Fig. 4, reveal two main mass modes, one at roughly 500 nm (particle diameter) and another around 1–2 μm. In the sample E3 this mode has shifted to larger sizes than in E1 and E2. One can also, systematically, detect a mass mode at around 200 nm in all of the event samples E1, E2 and E3, whereas, in the non-event samples such mode does not clearly exist. On the contrary, the non-event samples consist of a significant mass mode at 500–700 nm. The E2 sample seems to have a surprisingly low total mass concentration, only 2.6 μg/m^3. In order to get more complete picture of the mass size distribution we calculated the 3rd moment distribution using the average number size distributions presented in Fig 2. The resulting event and non-event 3rd moment size distributions are shown in Fig. 5. All

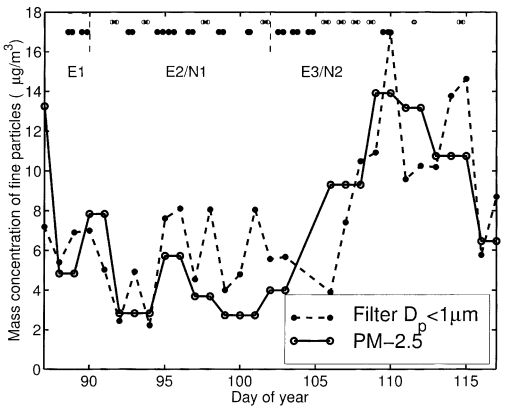

Fig. 3. Mass concentrations of fine particles determined by filter sampling ($Dp < 1$ μm) and the PM-2.5 determined by Dekati PM-10 impactor. The bars in the top row of the graph represent the event and non-event sampling periods by DLPI cascade impactor (as in Fig. 1).

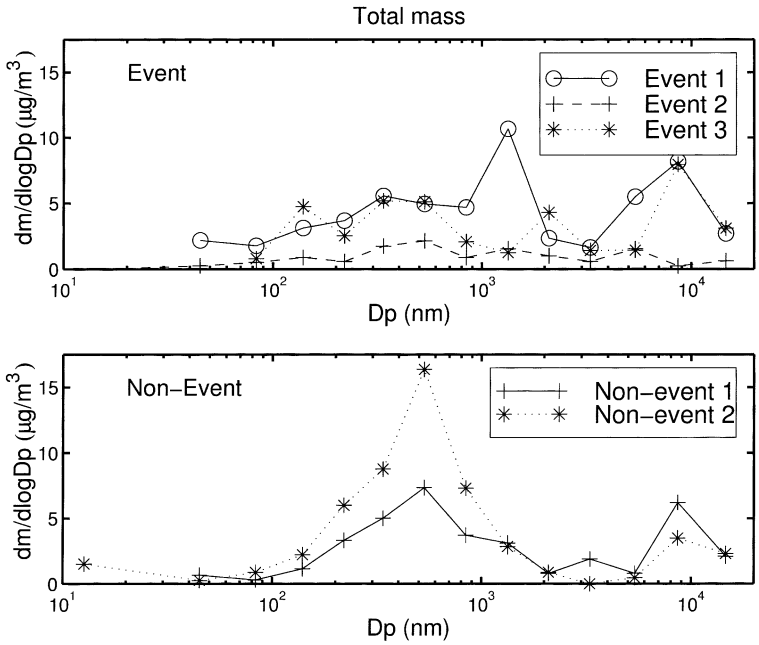

Fig. 4. Mass size distributions of different event and non-event samples obtained by DEKATI low pressure cascade impactor DLPI. The total volumes sampled in each case of E1, E2, E3, N1 and N2, were 23.3 m^3, 64.8 m^3, 57.2 m^3, 68.4 m^3 and 86.2 m^3, respectively (sampling times 13.6, 40.6, 35.8, 39,6 and 50.2 h).

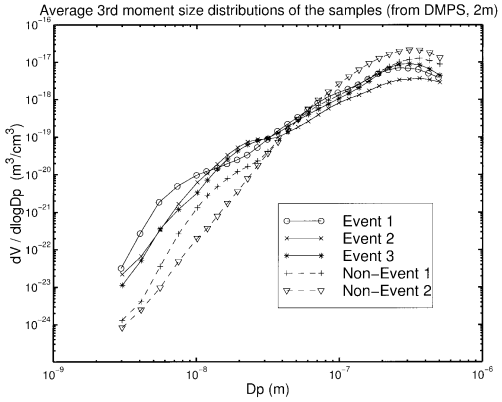

Fig. 5. Averaged submicron particle third moment size distributions during each cascade impactor sampling period. The spectra are calculated using the average number size distributions shown in Fig. 2.

the distributions show an accumulation mode at about 300 nm. Interestingly, the event distributions show also a nucleation/Aitken mode below 30 nm. It seems therefore possible that high quality impactor sampling could give information on the composition of the newly formed particles.

To get a rough estimate of the data quality and some support for further analysis, the mass concentrations of 5 different DLPI samples are compared with the corresponding estimated fine particle mass concentrations from filters and PM-10 impactors. It is summarized that the other two instruments show the same trend for the mass concentrations as the DLPI, especially that the event 2 sample has the lowest mass. This was already expected from the DMPS 3rd moment size distributions shown in Fig. 5. However, for the 2 event samples E2 and E3, the DLPI seems to give significantly lower mass concentrations than the other two instruments. This difference becomes explainable when the TEOM data is considered. In Fig. 6, the averaged mass concentration from TEOM for the event 2 period is shown as a function of time of day. There is a clear difference between the mass concentrations of early morning and afternoon. The reason for the decrease in the total mass concentration is most

probably dilution due to the vertical mixing during the nucleation event days. The mixing process has been observed to be connected with the nucleation burst, and is discussed elsewhere (Mäkelä et al., 2000; Kulmala et al., 2001). In Fig. 6, it is also seen that certain selected days from the E2 period show even a stronger dilution effect than the average curve. From this we conclude, that since the event samples are collected only on the afternoons of the nucleation burst days, the agreement between the full day samples by any instrument and the event samples cannot be completely fulfilled, at least if total mass is considered. It is therefore expected that the event samples should systematically give ($\sim$30%) lower mass concentrations than the full day samples.

6. Ionic concentrations and size distributions

The chemical analysis was done for several ionic species in aerosols. Since sodium is known to be non-volatile and to have no gaseous precursors in the atmosphere, we use sodium concentrations in the aerosol samples to test the consistency of the separate chemical methods. The consistency between the SDI and EMEP data is excellent for event 2, and the non-event samples. The SDI data for event 1 and event 3 periods was not available for sufficient number of days to be included into the comparison. However, we conclude that the SDI and EMEP samples were reasonably consistent.

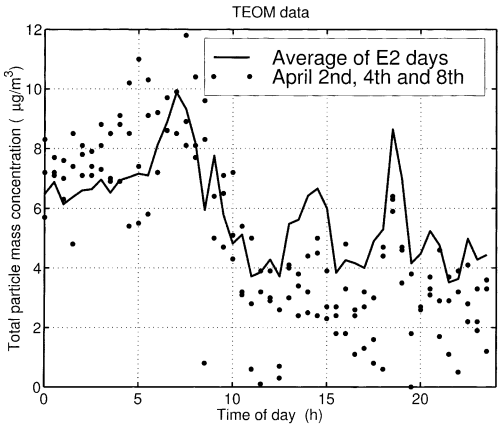

Fig. 6. TEOM data for total particle mass concentration as a function of time of day during event 2 sample period. The solid line refers to the average concentration for the event sample E2 days, and the dots refer to three separate days from the E2 period, namely 2, 4 and 8 April.

The size distributions of sulfate ions obtained by the ion chromatography for the DLPI impactor stages are presented in Figs. 7a, b. The particulate sulfate concentrations vary within the level 0.3–3 $\mu g/m^3$. Sulfate is mainly found in the accumulation mode with the peak maximum between 400 and 650 nm diameter. As a rule, the event samples show systematically lower sulfate concentrations than the non-event samples. Moreover, the difference between DLPI, SDI and EMEP data is large. The variation is assumed to partly arise from the fact that the samples have been taken in different time periods. Additionally some SO_2 from the gas phase may react with the samples during the collection.

For comparison we also estimated the ammonium concentrations in the three separate measurement systems. The data show that the ammonium concentrations obtained by the DLPI are once again, systematically lower that the other two. This is understandable, since the absolute mass concentrations are smaller in the DLPI samples as well. However, it also seen that the SDI data gives lower concentrations for ammonium than the EMEP filters. The ionic size distribution of ammonium shown in Figs. 8a, b reveals a peak at 400–600 nm, approximately the same sizes as for the sulfate.

The only actual comparable data on ionic concentrations are the daily SDI samples versus the daily EMEP samples. For an overall comparison between the SDI and EMEP data is presented in Fig. 9. In spite of the small differences between different ionic concentrations obtained, the event/non-event impactor data still look very similar for most of the compounds discussed so far. However, as seen in Fig. 10 in contrary to the non-event samples, the event samples show the presence of dimethylamine, a volatile organic base that behaves quite much like atmospheric ammonia. Ambient dimethylamine has been observed in several locations (Mosier et al., 1973; Tuazon et al., 1978) but its gas/particle partitioning is investigated mostly only in marine air (Gibb et al., 1999). The boiling point of dimethylamine is known to be 7.4°C and the reaction rate constant with hydroxyl radical 6.5×10^{-11} l/cm^{-3} s^{-1} (Gibb et al., 1999). The amines, as well as NH_3, are

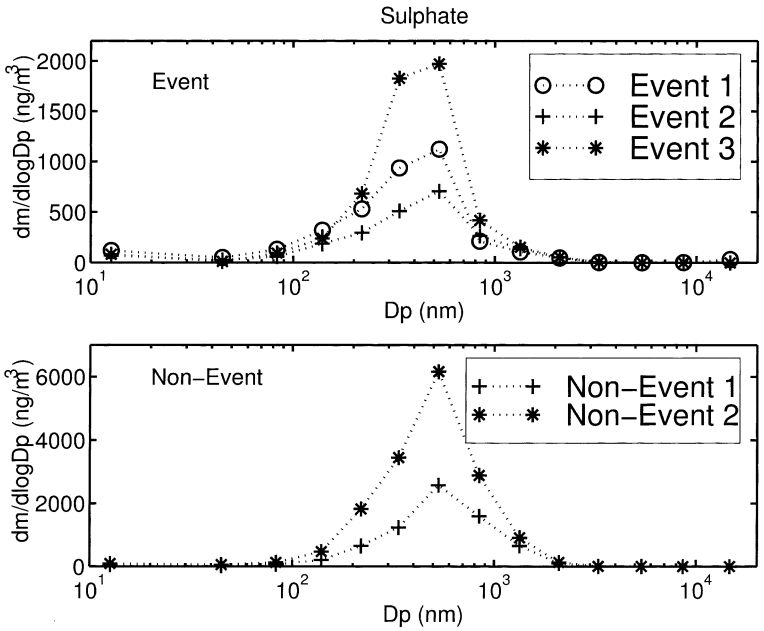

Fig. 7. Sulfate ion size distributions in the 5 different DLPI samples. Nucleation event samples (top) and non-event samples (bottom).

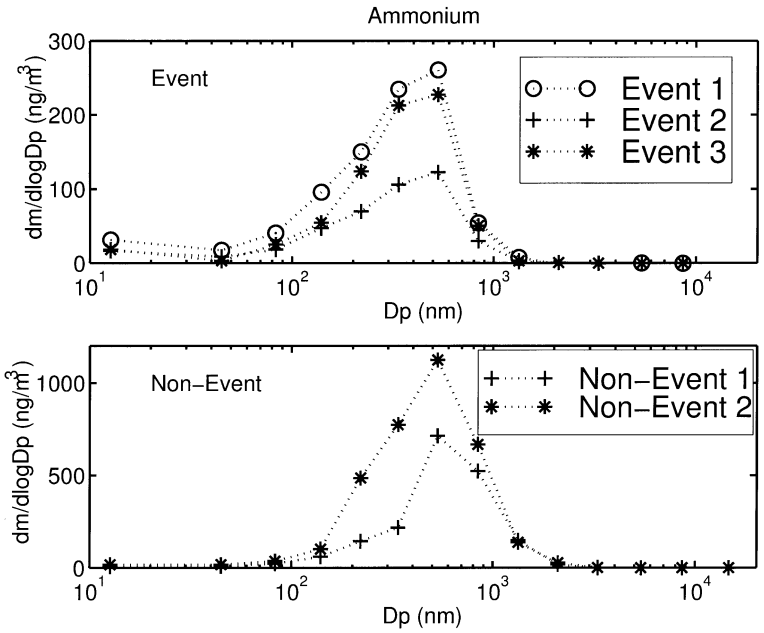

Fig. 8. Ammonium ion size distributions in the 5 different DLPI samples. Nucleation event samples (top) and non-event samples (bottom).

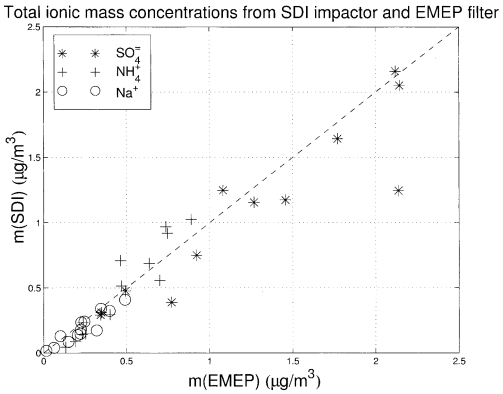

Fig. 9. Comparison of SDI and EMEP total concentration data for sulfate, ammonium and sodium ions.

known to be end products of the microbial turnover of labile organic matter. Also anthropogenic sources such as industrial activities, feedlot operations, waste incineration and sewage treatment are known to exist (Schade and Crutzen, 1995). Amines have also been measured in nonurban areas (Tanner and Eisele, 1991). From the multiple potential sources, it would be understandable that dimethylamine is abundant during most of the days in BIOFOR 3. The question is, why dimethylamine is transformed into the particulate phase only during particle formation event days? Very interestingly, the dimethylamine in BIOFOR 3 is very abundant in the event 3 sample even compared with E1 and E2 samples. Other methylamines (such as monomethylamine and trimethylamine) were not identified in the samples. However, some unidentified peaks were found in the chromatograms, suggesting that either of these may have been present in low concentrations.

After its production in the atmosphere, sulfuric acid is afterwards partially neutralized by ammonium and dimethylammonium. We have calculated the mass size distributions as ion charge equivalents for the samples E2 and N2. Here, also MSA and dicarboxylic acids (discussed later) are taken into account. The result suggests that the particles are still acidic. Therefore, it is probable that ammonium nitrate can not form for thermodynamic reasons (Saxena et al., 1986) and it is not observed, at least in the event 2 and non-event 2 samples. Nitrate found in the samples is most likely associated with the sea salt particles.

The size distributions of methanesulfate MSA^- have a maximum mode at the same sizes as the

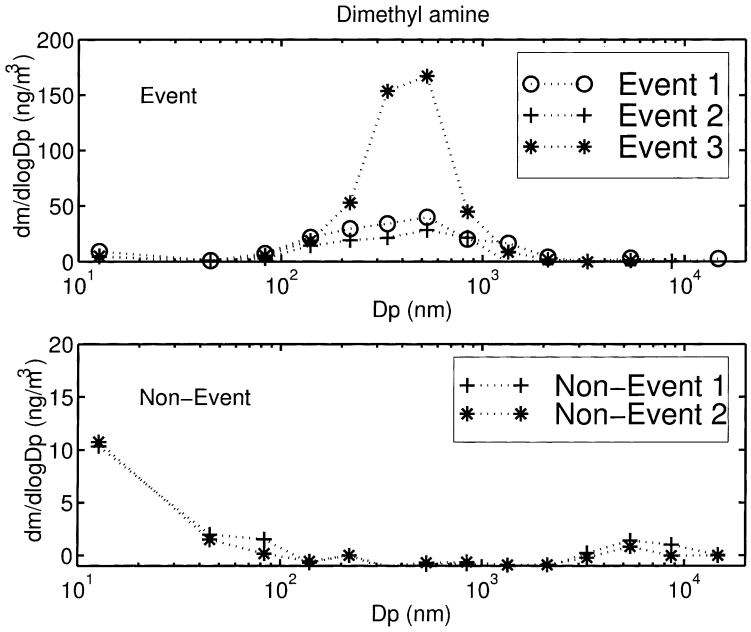

Fig. 10. Ionic size distributions of dimethylammonium, an ionic component of dimethylamine in the 5 different DLPI samples. Nucleation event samples (top) and non-event samples (bottom).

Table 3. *Comparison of total particle mass concentration and the fine particle mass concentration from the DLPI (during events/non-event afternoons) with the fine particle mass from the 2-stage filter collection (daily, 24 h samples noon-to-noon) and the PM-2.5 from the Dekati PM-10 impactor (2–3 day samples)*

Mass	DLPI total ($\mu g/m^3$)	DLPI fine ($\mu g/m^3$)	Filter fine ($\mu g/m^3$)	PM-2.5 ($\mu g/m^3$)
event 1	10.8	4.3	6.2	4.8
event 2	2.6	1.4	5.5	3.9
event 3	8.8	4.7	7.7	7.1
non-event 1	7.4	4.2	6.1	4.3
non-event 2	11.7	9.5	9.2	10.4

sulfate distributions. However, there seems to be no remarkable difference between the samples, even though the mass concentrations of the separate samples were different as seen in Table 3. The origin of MSA is assumedly maritime. It is assumed to be formed as a result of photochemical oxidation chain of dimethylsulfide (DMS) (Berresheim et al., 1995; Davis et al., 1998). Very interestingly, the event samples tend to have MSA in the nucleation mode fraction. It may be questioned whether this is a real aerosol result, or whether the MSA has condensed from the gas phase onto the back-up filter of the DLPI. However, it is probable that MSA is more abundant in the air masses arriving from North Atlantic which, in our case, means the event samples.

Table 4. *Technical info of the low pressure cascade impactors used in the study: #657 = "event impactor" DLPI; #678 = "non-event" impactor DLPI and #SDI daily impactor sampling. The volume flow rates were: #657: 26.60 l/min; #678: 28.64 l/min and #SDI: 11.0 l/min*

	#657	#657	#678	#678	#SDI
Stage	D50% (nm)	Geom. Dp (nm)	D50% (nm)	Geom. Dp (nm)	D50% (nm)
filter	—	9.8	—	9.5	—
1	32	44.9	30	42.8	—
2	63	83.2	61	80.4	86
3	110	140	106	134	153
4	177	219	169	209	231
5	272	337	259	321	343
6	417	530	399	508	591
7	674	841	647	808	796
8	1050	1336	1010	1283	1060
9	1700	2098	1630	2014	1660
10	2590	3294	2490	3167	2680
11	4190	5392	4030	5192	4080
12	6940	8629	6690	8317	8500
13	10 730	15 174	10 340	14 622	30 000

The light dicarboxylic acids oxalic, malonic, succinic acids were found in all the samples (in the form of organic ions). The concentrations in the non-event samples were systematically higher than in the event samples. Since the difference is of the order of 30–40%, it is assumed to be mostly due to the higher overall mass concentrations in the non-event samples. Apparently especially non-event oxalate and succinate coincide with the particle mass. Succinate seems to be present mostly in the fine particle fraction, whereas for oxalate and malonate, a coarse mode also exists. Malonate has a clearly bimodal distribution. This may be caused that it is split between the accumulation mode (sulfate particles) and the seasalt mode (sodium particles). The maxima of the malonate distribution coincide with the sulfate and sodium maxima. The other dicarboxylic acids (oxalic and succinic) are associated with the accumulation mode sulfate particles regardless of their low pH-value. The reason may be either due to the higher volatility of malonate than that of oxalate or succinate. Malonic acid is also more water soluble than the other two acids.

In addition to the carboxylic acids mentioned here, some other, probably organic acid anions were found in the chromatograms. It has to be noted, that there are several important organics, e.g. pinonic acids, that we are unable to identify or to quantify by this method.

To summarize the comparison between the event and non-event samples we present the mass

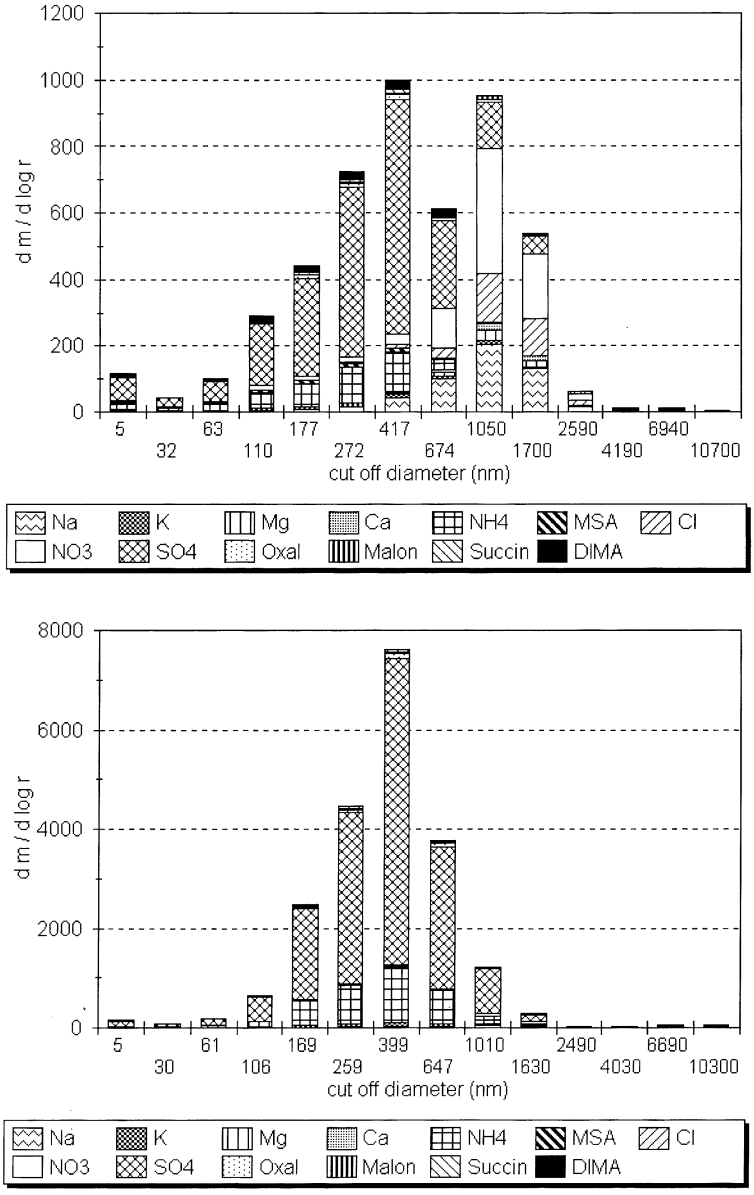

Fig. 11. Ionic mass concentrations for the event sample 2 (top), and for the non-event sample 2 (bottom).

distributions of the most abundant ions measured in the samples E2 and N2 in Figs. 11a, b.

7. Conclusions

In this study, the chemical composition of the aerosol during and subsequent to the ambient particle formation process has been studied. The mass related data suggests that, the total particle mass concentrations were systematically lower when particle formation occurred. All the other results on mass are fairly consistent and we may derive some conclusions based on the data obtained within BIOFOR 3 campaign.

Partly because of the lower overall mass concen-

trations, the particle formation event aerosol data showed lower sulfate concentrations than the reference data. In the event samples also nucleation mode particle MSA (methanosulphonic acid) was found to be present. This may be a consequence of the events showing preference for air masses arriving from Northern Atlantic. The sea salt mode was also more pronounced in the event samples indicating the connection of the event preferring conditions towards marine air masses. MSA is known to be a reaction product of DMS, which is of maritime biological origin. It is not clear why the MSA concentration in the Aitken and accumulation modes were practically equal in all the samples and only in the nucleation mode fraction the excess of MSA was observed.

For the organic diacids analyzed, the obtained concentrations were systematically higher for the non-event samples. This agrees with the general difference in total mass concentrations.

The event samples show significant presence of dimethylammonium compared to the non-event samples. Thus, the measurements have shown the presence of an ionic component of dimethylamine in the particulate phase during and/or shortly after the particle formation events. If one takes into account that the event aerosol had roughly 30–40% lower total mass concentrations, the relative difference between the event and non-event aerosol dimethylamine is approximately 50-fold. As the measurements have shown dimethylamine to be correlated with sulfate, two salts may be considered: dimethylammonium sulfate $((CH_3)_2NH_2)_2SO_4$ and dimethylammonium bisulfate $(CH_3)_2NH_2HSO_4$. The observation of particulate dimethylamine presence during the nucleation bursts also partly supports the discussion by Bigg (2001) about the organic origin of the nucleation agents. However, further conclusions need more accurate measurements of the gas phase species.

8. Acknowledgements

The financial support from the European Commission Environment and Climate Programme under contract ENV4-CT97-0405 (BIOFOR) and national support from Maj and Tor Nessling foundation (project nos. 98173 and 99109) is gratefully acknowledged. We would also like to thank the personnel of SMEAR II station and Hyytiälä Forestry Field Station for continuous support during the project. We thank especially Dr. Winifried Seidl who passed away in August 2000.

REFERENCES

Berresheim, H., Wine, P. H. and Davis, D. D. 1995. Sulfur in the atmosphere. In: *Composition, chemistry, and the climate of the atmosphere* (ed. H. B. Singh), pp. 251–307. Van Nostrand Reinhold, New York.

Bigg, E. K. 2001. The aerosol in a boreal forest in spring. *Tellus* **53B**, 510–519.

Davis, D., Chen, G., Kasibhatla, P., Jefferson, A., Tanner, D., Eisele, F., Lenschow, D., Neff, W. and Berresheim, H. 1998. DMS oxidation in the Antarctic marine boundary layer: comparison of model simulations and field observations of DMS, DMSO, $DMSO_2$, H_2SO_4(g), MSA(g), and MSA(p). *J. Geophys. Res.* **103**, 1657–1678.

Gibb, S. W., Mantoura, R. F. C. and Liss, P. S. 1999. *Global Biochemical Cycles* **13**, 161–178.

Jaffrezo, J.-L., Calais, N. and Bouchet, M. 1998. Carboxylic acids measurements with ionic chromatography. *Atmos. Environ.* **32**, 2705–2708.

Kavouras, I. G., Mihalopoulos, N. and Stephanou, E. G. 1998. Formation of atmospheric particles from organic acids produced by forests. *Nature* **395**, 683–686.

Kerminen, V.-M., Teinilä, K., Hillamo, R. and Mäkelä, T. 1999. Size-segregated chemistry of particulate dicarboxylic acids in the Arctic atmosphere. *Atmos. Environ.* **33**, 2089–2100.

Kulmala, M., Toivonen, A., Mäkelä, J. M. and Laaksonen, A. 1998. Analysis of the growth of nucleation mode particles observed in Boreal forest. *Tellus* **50B**, 449–462.

Kulmala, M., Hämeri, K., Aalto, P. P., Mäkelä, J. M., Pirjola, L., Nilsson, E. D., Buzorius, G., Rannik, Ü., Dal Maso, M., Seidl, W., Hoffmann, T., Janson, R., Hansson, C.-H., Viisanen, Y., Laaksonen, A. and O'Dowd, C. D. 2001. Overview of the international project on Biogenic aerosol formation in the boreal forest (BIOFOR). *Tellus* **53B**, 327–343.

Maenhaut, W., Hillamo, R., Mäkelä, T., Jaffrezo, J.-L., Bergin, M. H. and Davidson, C. I. 1996. A new cascade impactor for aerosol sampling with subsequent PIXE analysis. *Nucl. Instr. Meth. in Phys. Res.* **B 109/110**, 482–487.

Mosier, A. R., Andre, C. E. and Viets, F. G., Jr. 1973. *Environ. Sci. Technol.* **7**, 642–644.

Mäkelä, J. M., Aalto, P., Jokinen, V., Pohja, T., Nissinen, A., Palmroth, S., Markkanen, T., Seitsonen, K., Lihavainen, H. and Kulmala, M. 1997. Observations

of ultrafine aerosol particle formation and growth in boreal forest. *Geophys. Res. Lett*. **24**, 1219–1222.

Mäkelä, J. M., Dal Maso, M., Laaksonen, A., Kulmala, M., Pirjola, L., Keronen, P. and Laakso, L. 2000. Characteristics of the aerosol particle formation events observed at a boreal forest site in southern Finland. *Borealis Environment Research* **5**, 299–313.

Nilsson, E. D., Paatero, J. and Boy, M. 2001. Effects of air masses and synoptic weather on aerosol formation in the continental boundary layer. *Tellus* **53B**, 441–461.

O'Dowd, C. D, McFiggans, G., Creasey, D. J., Pirjola, L., Hoell, C., Smith, M. H., Beverley, J. A., Plane, J. M., Heard, D. E., Lee, J. D., Pilling, M. and Kulmala, M. 1999. On the photochemical production of biogenic new particles in the coastal boundary layer. *Geophys. Res. Lett*. **26**, 1707–1710.

Saxena, P., Hudischewskyj, A. B., Seigneur, C. and Seinfeld, J. 1986. A comparative study of equilibrium approaches to the chemical characterization of secondary aerosols. *Atmos. Environ.* **20**, 1471–1483.

Schade, G. W. and Crutzen, P. J. 1995. Emission of aliphatic amines from animal husbandry and their reactions: Potential source of N_2O and HCN. *J. Atmos. Chem.* **22**, 319–346.

Tanner, D. J. and Eisele, F. L. 1991. Ions in oceanic and continental air masses. *J. Geophys. Res.* **96**, 1023–1031.

Teinilä, K., Kerminen, V.-M. and Hillamo, R. 2000. A study of size-segregated aerosol chemistry in the antarctic atmosphere. *J. Geophys. Res.* **105**, 3893–3904.

Tuazon, E. C., Winer, A. M., Graham, R. A., Schmid, J. P. and Pitts, J. N., Jr. 1978. *Environ. Sci. Technol.* **12**, 954–958.

Weber, R. J., Marti, J. J., McMurry, P. H., Eisele, F. L., Tanner, D. J. and Jefferson, A. 1997. Measurements of new particle formation and ultrafine particle growth rates at a clean continental site. *J. Geophys. Res.* **102**, 4373–4385.